ISSN 1990-4789, Journal of Applied and Industrial Mathematics, 2023, Vol. 17, No. 4, pp. 750–759. © Pleiades Publishing, Ltd., 2023.
Russian Text © The Author(s), 2023, published in Sibirskii Zhurnal Industrial'noi Matematiki, 2023, Vol. 26, No. 4, pp. 65–76.

Influence of Mathematical Model Parameters on Plasma Transfer in a Helical Magnetic Field

G. G. Lazareva[1*], I. P. Oksogoeva[1], and A. V. Sudnikov[2***]**

[1] *RUDN University, Moscow, 117198 Russia*

[2] *Budker Institute of Nuclear Physics, Siberian Branch, Russian Academy of Sciences, Novosibirsk, 630090 Russia*

*e-mail: *lazareva-gg@rudn.ru, **oksogi@mail.ru, ***a.v.sudnikov@inp.nsk.su*

Received May 16, 2023; revised October 17, 2023; accepted November 1, 2023

Abstract—The paper presents the results of mathematical modeling of plasma transfer in a helical magnetic field using new experimental data obtained at the SMOLA trap created at the Budker Institute of Nuclear Physics of the Siberian Branch of the Russian Academy of Sciences. Plasma is confined in the trap by transmitting a pulse of magnetic field with helical symmetry to the rotating plasma. The mathematical model is based on a stationary plasma transfer equation in the axially symmetric formulation. The distribution of the concentration of the substance obtained by numerical simulation confirmed the confinement effect obtained in the experiment. The dependences of the integral characteristics of the substance on the depth of magnetic field corrugation and on plasma diffusion and potential are obtained. The numerical implementations of the model by the relaxation method and by the Seidel method are compared.

Keywords: *mathematical modeling, transfer equation,helical magnetic field*

DOI: 10.1134/S1990478923040063

INTRODUCTION

Studies of plasma flow in a magnetic field are of considerable interest for controlled thermonuclear fusion [1], investigating the resistance of materials under the influence of powerful thermal loads [2], laboratory modeling of astrophysical processes [3], and a number of other fundamental and applied scientific problems. To solve problems of controlled thermonuclear fusion, it is necessary to contain high-temperature plasma of sufficient density in a limited region of space. For a positive energy yield, the product of plasma density and energy lifetime must exceed a threshold value (for a mixture of deuterium and tritium $n\tau \sim 10^{20}$ s/m^3, for pure deuterium $n\tau \sim 10^{22}$ s/m^3) [4]. Increased lifetime is achieved by reducing energy losses from the confinement area. The main method of plasma thermal insulation considered today is its confinement in a magnetic field of various configurations [1]. The greatest progress has been achieved in systems with a toroidal magnetic field topology. An alternative approach is plasma confinement in open magnetic systems, where the field is close to axisymmetric and its field lines intersect the boundary of the confinement domain at two points [5]. The advantages of this approach are more efficient use of magnetic field energy, as well scalability and engineering simplicity of the system. The main scientific goal of open trap physics is to reduce the loss of particles and energy along magnetic field lines in the regions where they leave the confinement region.

Great progress has been made in understanding the physics of open magnetic configurations and the achieved plasma parameters [6]. To date, a number of possible solutions of the longitudinal confinement problem have been proposed and experimentally tested, including suppression of longitudinal losses by a periodic magnetic field (multimirror confinement) [5]. Plasma confinement by a magnetic field with helical symmetry was proposed as a development of the multimirror confinement method [7]. In the reference frame of the rotating plasma, the movement of magnetic

disturbances has a velocity component codirectional with the magnetic field, which allows momentum to be transferred to the trapped particles. Collisions between transient and trapped particles provide an effective force acting on the plasma as a whole and facilitating the return of ions to the confinement region. The SMOLA (from Russian 'Spiral Magnetic Open Trap') installation was developed and built in 2017 at the Budker Institute of Nuclear Physics of the Siberian Branchc of the Russian Academy of Sciences for experimental testing of this idea [8, 9]. In the SMOLA installation, the area in which plasma is contained is limited on one side by a classic cork and on the other side by a multimirror section with a helical magnetic field. In the experiment, parameters such as the longitudinal magnetic field, the ratio of the longitudinal and helical magnetic fields, and the density and rotation speed of plasma are varied. The SMOLA facility is designed to simulate the effects of helical confinement at a low (and therefore easily achievable) plasma temperature. To scale helical confinement on a thermonuclear-class system, a detailed comparison of experimentally observed matter flows with model ones and further calculation of the efficiency of a larger-scale system based on the mathematical model are necessary. Currently, the observed results have been shown to correspond to approximate theoretical estimates. At the same time, an exact analytical solution for the theory of helical confinement has not been constructed, so the comparison can be based on the results of a numerical solution of the equations of plasma motion.

A mathematical model of transfer of matter in a helical magnetic field is constructed based on equations in [7, 10] and SMOLA installation parameters. Mathematical modeling of the process was carried out for the first time in [11]. The purpose of this work is to validate the model and optimize the experimental parameters.

1. STATEMENT OF THE PROBLEM

Let us consider the motion of plasma in the central part of a cylinder-shaped trap (see Fig. 1). The matter enters the confinement region from the plasma source through the left end of the cylinder and exits into the expander through the right boundary. Let us consider the cross section of a cylinder in the plane (r, z). In the paper [12], expressions were obtained for the components of radial and longitudinal transport of particles in a helical magnetic field. The system of equations describes the dynamics of plasma in the MHD approximation in an axially symmetric formulation. Differences in the motion of trapped and transient ions are taken into account in the form of an effective friction force that depends on the mutual velocity of the components and the fraction of the trapped particles. The longitudinal force acting on the plasma arises as a result of the interaction of the radial electric current of the trapped ions with the azimuthal component of the helical magnetic field. Plasma diffusion across the magnetic field is taken into account. Elimination of dependent

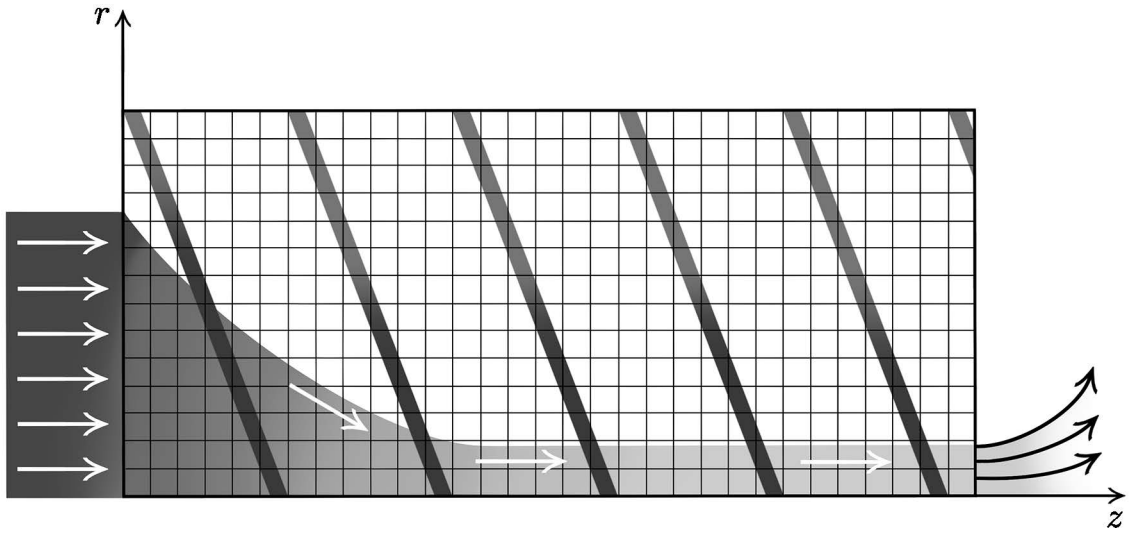

Fig. 1. Diagram of the central part of the trap.

variables reduces the system of equations to the flow continuity equation

$$l\frac{\partial}{\partial z}\frac{1}{\Lambda}\frac{\partial(Tu)}{\partial z}+l\big(1+\kappa(r)\big)\kappa(r)\frac{\partial u}{\partial z}\left(\zeta(r)\frac{\partial\phi(r)}{\partial r}\right)+\kappa(r)\frac{\partial}{\partial r}l\frac{1}{Z}\zeta(r)\frac{\partial(Tu)}{\partial z}+\kappa(r)\frac{\partial}{\partial r}lD\frac{\partial u}{\partial r}=0, \tag{1}$$

where u is the concentration of the substance, $T=T_i+T_e$, $T_i=4$ eV and $T_e=30(1-(r/r_0)^2)$ are the ion and electron temperatures, Λ is the ratio of the length of the system to the mean free path λ, $\kappa(r,R_m)$ is the fraction of trapped particles, $l=216$ cm is the length of the system along the field line, Z is the average charge of one ion, and D is the diffusion coefficient in the transverse field. The fraction of trapped particles $\kappa(r,R_m)=1-1/R(r,R_m)$, $R(r,R_m)=2(R_m-1)(r/a)^2+1$, where $R_m=1.52$ is the corrugation depth. The parameter $\zeta=c/V_z$ is the ratio of the speed of sound $c_s=(T_e/M)^{1/2}$ to the longitudinal velocity V_z of motion of magnetic disturbances under rotation of plasma in its own ambipolar electric field. In Eq. (1), the physical variables are made dimensionless by normalization to $r_0=a$, $z_0=l$, $\phi_0=T_e/e$, $u_0=u_{\max}$, and $T_0=T_e$, where $a=8$ cm is the boundary of the chamber in which plasma can exist. The electric field potential $\phi(r)$ is introduced as a polynomial that interpolates experimental data [13],

$$\phi(r)=-2.21776+1.31r-7.79r^2+31.18r^3-33.43r^4+10.94r^5.$$

In the simulated experiment, the plasma and electromagnetic field parameters are settled within 40 ms and then a phase begins when the process is steady for 120 ms, after which the discharge is turned off. The main task of experiments and mathematical modeling is to study plasma confinement in which all parameters remain constant. The plasma potential measured using probes in experiments on the SMOLA installation depends on the experimental parameters. The maximum of ϕ varies from $2T_e/e$ to $3T_e/e$. The maximum value of the dimensionless potential ϕ for the next generation of installations, in which it is possible to use the principle of helical confinement, also lies within the same limits [14, 15]. The experimentally observed potential distribution in the central region of the plasma (for radius values less than 0.6 in dimensionless quantities) is close to quadratic; further, in the peripheral region of the plasma, the derivative of the potential with respect to radius decreases. The error in measuring the potential in the experiment is approximately 5 %. The degree and coefficients of the approximating polynomial are selected in such a way that its deviation from the values experimentally measured in the reference experiment is comparable to the experimental error.

To specify the influence of the field in the radial direction, the model uses the derivative of the absolute value of the electric field

$$q(r)=\frac{\partial\big|\phi(r)\big|}{\partial r}=|1.31-7.79r+31.18r^2-33.43r^3+10.94r^4|.$$

It is well known that the potential value decreases with increasing z due to the presence of transverse plasma conductivity. The spatial potential distribution is given as follows:

$$\Phi(r,z)=\left(1-\frac{0.002z}{h}\right)q(r).$$

Let us consider the domain $[0,r_{\max}]\times[0,z_{\max}]$ in the cross section of the central part of the installation (Fig. 1). In dimensionless quantities, the domain is a unit square. We assume that the matter does not reach the walls of the trap, we set a symmetry condition on the z-axis, and at the input and output of the substance we set the boundary distribution of the concentration of the substance $u(r,0)=u^L(r)$ and $u(r,z_{\max})=u^R(r)$, respectively. For the calculations, we used the experimental data [6] for the distribution of concentration at the boundaries. Figure 2b shows the experimental values of plasma concentration and their interpolation of the form

$$u^L(r)=1.03+0.46r-1.52r^2+14.48r^3-44.17r^4+43.77r^5-14.05r^6,$$

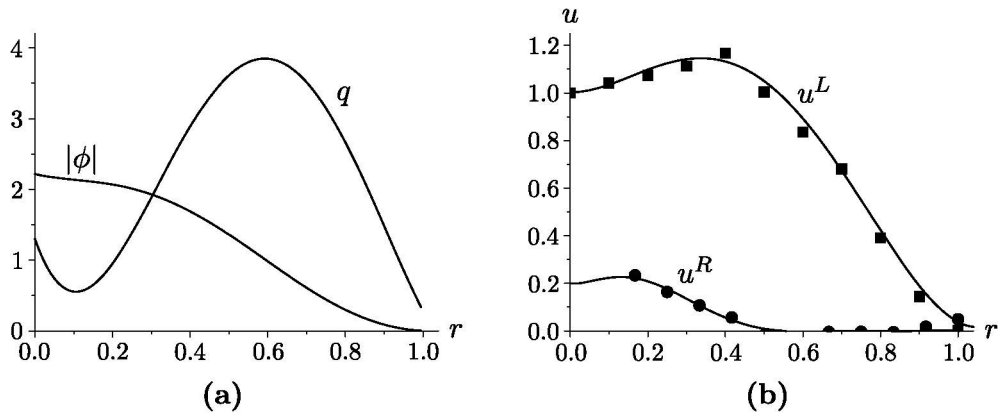

Fig. 2. Dependences of the modulus of the electric field potential and its derivative (a) and the boundary plasma distribution (b) on the installation radius at the input (squares) and output (circles).

$$u^R(r) = 0.2 - 0.12r + 9.11r^2 - 73.43r^3 + 210.13r^4 - 285.64r^5 + 188.54r^6 - 48.78r^7.$$

Thus, the steady-state problem has the form

$$C^1(r)\frac{\partial^2 u(r,z)}{\partial z^2} + C^2(r)\frac{\partial\big(\Phi(r,z)u(r,z)\big)}{\partial z} + C^3(r)\frac{\partial}{\partial r}C^4(r)\frac{\partial u(r,z)}{\partial z} + C^5(r)\frac{\partial^2 u(r,z)}{\partial r^2} = 0,$$
$$\frac{\partial u}{\partial r}(0,z) = 0, \quad u(r,0) = u^L(r), \quad \frac{\partial u}{\partial r}(1,z) = 0, \quad u(r,1) = u^R(r), \tag{2}$$

where the coefficients in the equation are

$$C^1(r) = lT(r)/\Lambda,$$
$$C^2(r) = l\big(1+\kappa(r)\big)\kappa(r)\zeta(r),$$
$$C^3(r) = \kappa(r),$$
$$C^4(r) = l\zeta(r)T(r)/Z,$$
$$C^5(r) = lD\kappa(r).$$

2. SOLUTION METHOD

The paper [11] implements the relaxation method [12]. The choice of this approach was determined by the reliability of the method and the ease of monitoring the correctness of the solution. The present paper presents an implementation of problem (2) using the more economical Seidel method. During the calculations, it turned out that the choice of stencil when approximating the mixed derivative affects the solution. When using the grid operator for the mixed derivative on a four-point [11] and six-point [13] stencil, $\Lambda_{rz} = C^3(r)(C^4(r)u_{\bar z})_r$ and $\Lambda_{rz} = C^3(r)(C^4(r)(u_{\bar z} + u_z)/2)_r$, oscillations occurred when the diffusion coefficient D dropped below 0.001. Here u_z and $u_{\bar z}$ are the forward and backward difference derivatives. Therefore, both solution methods (the relaxation method and the Seidel method) required careful selection of a stencil for approximating the mixed derivative $\kappa(r)\frac{\partial}{\partial r}\frac{l\zeta(r)T(r)}{Z}\frac{\partial u(r,z)}{\partial z}$ by finite differences. When using the operator [16]

$$\Lambda_{rz} = C^3(r)\Big((C^4(r)u_{\bar z})_r + \big(C^4(r)u_r\big)_{\bar z}\Big)/2,$$

no oscillations occur.

On a grid with nodes $r_i = ih$, $i = 1,\dots,N_r$, $z_k = kh$, $k = 1,\dots,N_z$, the grid functions $u^n_{i,k} = (u(r_i,z_k))^n$, $\Phi_{i,k} = \Phi(r_i,z_k)$, $C^1_i = C^1(r_i)$, $C^2_i = C^2(r_i)$, $C^3_i = C^3(r_i)$, $C^4_i = C^4(r_i)$, $C^5_i = C^5(r_i)$, $u^L_i = u^L(r_i)$, $u^R_i = u^R(r_i)$. The convergence criterion $|u^{n+1}_{i,k} - u^n_{i,k}| \le \varepsilon$, $\varepsilon = 10^{-8}$.

To implement problem (2) using the relaxation method for $\tau = 10^{-4}$, we used an unconditionally stable stabilizing correction scheme and the tridiagonal matrix algorithm [17]. The new version of the difference scheme has the form

$$\begin{gathered}\frac{u^*_{i,k}-u^n_{i,k}}{\tau} = C^1_i(u^*_{i,k+1}-2u^*_{i,k}+u^*_{i,k-1})/h^2 + C^2_i(\Phi_{i,k+1}u^*_{i,k+1}-\Phi_{i,k-1}u^*_{i,k-1})/2h \\ + C^3_i\Big(C^4_{i+1/2}(u^n_{i+1,k}-u^n_{i,k}-u^n_{i+1,k-1}+u^n_{i,k-1}) \\ + C^4_{i-1/2}(u^n_{i,k+1}-u^n_{i,k}-u^n_{i-1,k+1}+u^n_{i-1,k})\Big)/2h^2 \\ + C^5_i(u^n_{i+1,k}-2u^n_{i,k}+u^n_{i-1,k})/h^2, \\ i=1,\dots,N_r, \quad k=2,\dots,N_z-1, \quad u^*_{1,k}=u^*_{2,k}, \quad u^*_{N_r,k}=u^*_{N_r-1,k}, \\ \frac{u^{n+1}_{i,k}-u^*_{i,k}}{\tau} = C^1_i(u^{n+1}_{i+1,k}-2u^{n+1}_{i,k}+u^{n+1}_{i-1,k})/h^2 - C^1_i(u^n_{i+1,k}-2u^n_{i,k}+u^n_{i-1,k})/h^2, \\ i=2,\dots,N_r-1, \quad k=1,\dots,N_z, \quad u^{n+1}_{i,1}=u^L_i, \quad u^{n+1}_{i,N_z}=u^R_i.\end{gathered} \tag{3}$$

Solving Eq. (2) using the Seidel method [18] at each time step allows one to construct an economical algorithm. The difference scheme based on the Seidel method has the form

$$\begin{gathered}u^{n+1}_{i,k} = (\beta^1_+u^n_{i+1,k}+\beta^1_-u^{n+1}_{i-1,k}+\beta^2_+u^n_{i,k+1}+\beta^2_-u^{n+1}_{i,k-1}+\beta^3_+u^n_{i+1,k-1}+\beta^3_-u^n_{i-1,k+1})/\beta, \\ \beta = 2(C^1_i+C^5_i)+C^3_i(C^4_{i+1/2}+C^4_{i-1/2})/2, \\ \beta^1_\pm = C^5_i+(C^3_iC^4_{i\pm1/2})/2, \\ \beta^2_\pm = C^1_i \pm (hC^2_i\Phi_{i,k\pm1}+C^3_iC^4_{i\mp1/2})/2, \\ \beta^3_\pm = -(C^3_iC^4_{i\pm1/2})/2, \\ i=2,\dots,N_r-1, \quad k=2,\dots,N_z-1, \quad u^{n+1}_{1,k}=u^{n+1}_{2,k}, \\ u^{n+1}_{N_r,k}=u^{n+1}_{N_r-1,k}, \quad u^{n+1}_{i,1}=u^L_i, \quad u^{n+1}_{i,N_z}=u^R_i.\end{gathered} \tag{4}$$

It can be noted that the problem (3) and the solution algorithm (4) contain the parameter $\zeta(r) = 1/Ar$, obtained by approximating the experimental data; here $A = 20$. On the axis for $r = 0$, the parameter ζ is limited to the value for $r = \rho_B$, where $\rho_B = V_{T_i} \cdot mc/eB$ is the gyroradius. For the SMOLA installation parameters $\rho_B \approx 0.3$–0.4 cm. This is due to the fact that the ion moves along a Larmor orbit (rotates in a magnetic field), and therefore, its radial coordinate oscillates. In the model under consideration, all influences are averaged, and the ion is assigned the coordinate of the center of the circle along which it moves in the magnetic field. That is, the coordinate is equal to zero for ions that fly around the axis and are at a distance of the gyroradius from it. Therefore, to eliminate the singularities of the solution during calculations in the vicinity of the symmetry axis, the dimensionless parameter ζ is specified as follows:

$$\zeta(r) = \begin{cases} 1/Ar & \text{if} \quad r > \rho_B \\ 1/A\rho_B & \text{if} \quad \rho_B \geq r \geq 0. \end{cases}$$

Along with other advantages, the Seidel method is interesting for its ease of use in cylindrical coordinates. The principle of expressing the required element in terms of scheme-neighboring points of the "cross" type is universal and independent of the choice of coordinate system.

3. NUMERICAL SIMULATION RESULTS

For the test problem, we consider the equation

$$\begin{gathered}\frac{\partial^2u}{\partial z^2}+\frac{\partial^2u}{\partial r^2}+\frac{\partial^2u}{\partial z\partial r}-\frac{\partial^2u}{\partial r\partial z}=0, \\ u(r,0)=0, \quad u(0,z)=0, \quad u(r,1)=\sin\left(\frac{5\pi r}{2m}\right), \quad \frac{\partial u}{\partial r}(m,z)=0.\end{gathered} \tag{5}$$

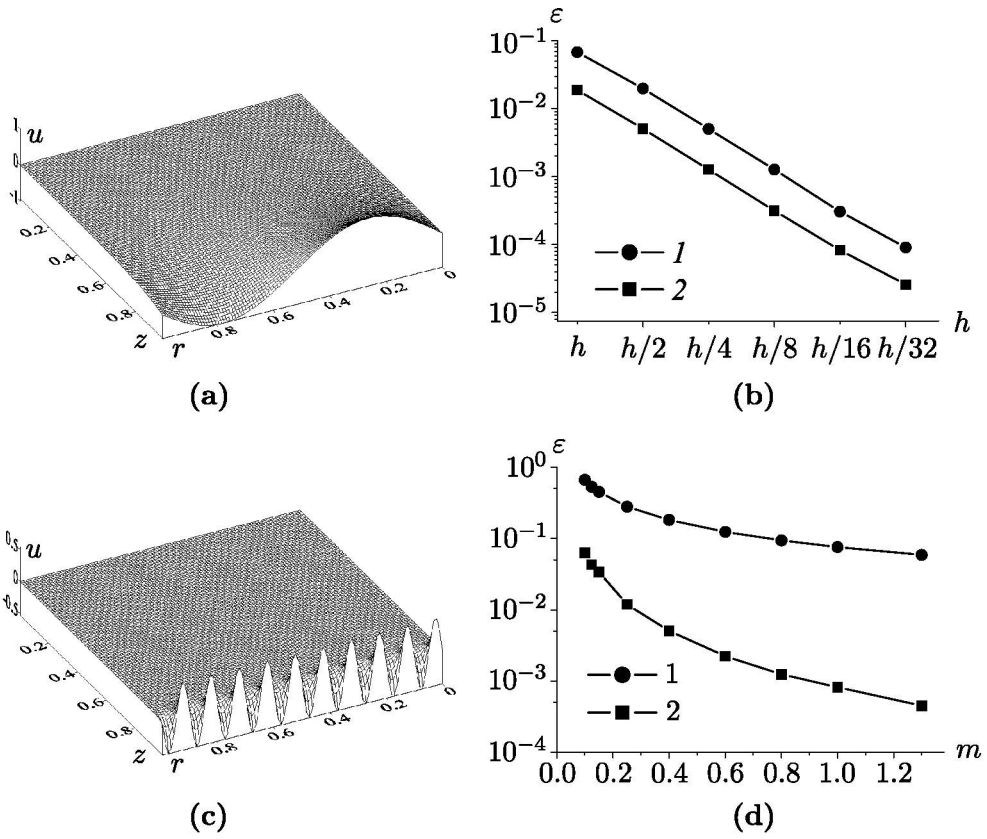

Fig. 3. Distribution of the test problem solution function for $m = 1.3$ (a) and $m = 0.124$ (c); graph of the accuracy of convergence to the solution depending on the grid step (b) and the problem parameter m (d) when using the relaxation method (circles) and the Seidel method (squares).

Problem (5) has the analytic solution (Fig. 3a)

$$u_{ex}(r,z) = \frac{\exp\left(\frac{5\pi}{2m}z\right) - \exp\left(-\frac{5\pi}{2m}z\right)}{\exp\left(\frac{5\pi}{2m}\right) - \exp\left(-\frac{5\pi}{2m}\right)} \sin\left(\frac{5\pi r}{2m}\right).$$

Approximation of mixed derivatives in Eq. (5) by finite differences yields a result depending on the order of differentiation with respect to coordinates,

$$\Lambda_{rz} = \big((u_{\bar{r}})_z + (u_r)_{\bar{z}}\big)/2,$$
$$\Lambda_{zr} = \big((u_z)_r + (u_{\bar{z}})_{\bar{r}}\big)/2.$$

We obtained graphs (Fig. 3b) of the relative error $\varepsilon = \frac{\|u^{n+1}-u_{ex}\|}{\|u_{ex}\|}$ to achieve criterion for the convergence of the iterative process $\varepsilon_n = 10^{-8}$ on a sequence of refined meshes. The Seidel method is more economical and easier to implement than the relaxation method. The required number of iterations of the relaxation method exceeds 4000. The Seidel method requires up to a thousand iterations, and in the case of the proposed stencil for approximating the mixed derivative, convergence occurs twice as fast. As the coefficient m of the boundary condition in problem (5) decreases, the number of complete periods of the sine function on the boundary increases (Figs. 3a, 3c). As the number of grid points per sine period increases, a uniform exponential decrease in error of the form $\varepsilon = A_0^m + A_1^m \exp(-m/m_1) + A_2^m \exp(-m/m_2)$ is observed (Fig. 3d). As m increases, the convergence rate of each method increases. For example, when $m = 0.124$, 10 radial grid points are

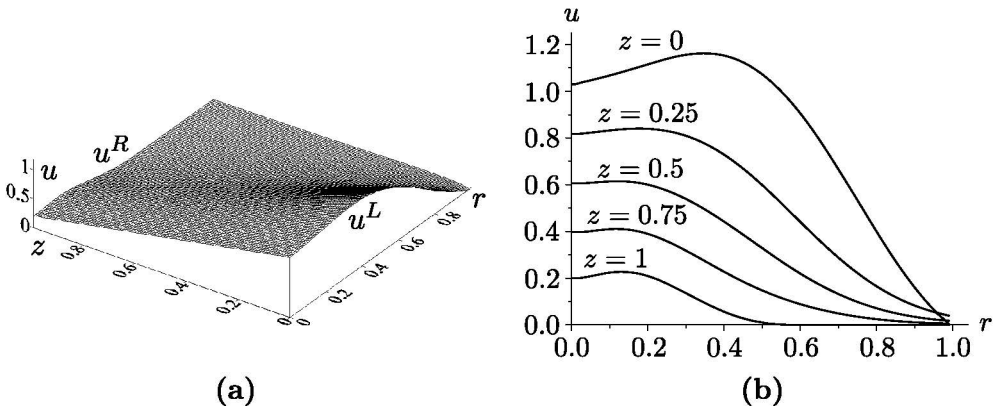

Fig. 4. Plasma concentration distribution in a helical magnetic field (a) and matter concentration along sections of the z-axis (b).

used to calculate the total sine period (Fig. 3c). For $m = 1.3$, the full period (Fig. 3a) occupies the entire boundary of the computational domain (100 points) and the convergence rate of each method is twice as high compared as that with $m = 0.124$.

In the course of modeling the transfer of matter in a helical magnetic field, concentration distributions were obtained for various values of the magnetic field corrugation depth, diffusion, and plasma potential. The plasma concentration distribution is shown in a computational domain that has the shape of a unit square in dimensionless form (Fig. 4a). Sections along the z-axis are given (Fig. 4b) for further analysis of the calculation results and comparison with experimental data. Calculations show a decrease in plasma density; this confirms the confinement effect observed in experiments.

Since there are experimental data available on the plasma concentration in the cross section $z = 0.4$, the results of calculations are presented only in this section (Fig. 5). Computational experiments were carried out for various permissible values of the diffusion coefficient, the derivative of the absolute value of the electric field, and the corrugation depth. For further use of the model, the calculation of the integral of density over the cross section, $I(z) = \int_0^1 u(r, z)\, dr$, was introduced.

Calculations have shown that as the diffusion coefficient in the transverse field decreases, the matter begins to squeeze up against the axis (Fig. 5a). The coincidence of the calculated distributions with the experimental ones, taking into account the finite accuracy of the experimental changes, is achieved with a diffusion coefficient in the range $D = 0.01$–0.1. Further calculations were carried out with $D = 0.1$. Compression of the plasma pinch towards the axis is observed with an increase in the derivative of the absolute value of the electric field and the corrugation depth. The results obtained are consistent with the experimental data.

To predict the results of the operation of designed installations for confining plasma in a helical magnetic field, it is necessary to determine the diffusion coefficient more accurately. For this purpose, it is planned to carry out calculations with low values of the plasma potential using Neumann boundary conditions and experimental data obtained with the SMOLA installation at the Budker Institute of Nuclear Physics of the Siberian Branch of the Russian Academy of Sciences.

CONCLUSIONS

The paper presents the results of mathematical modeling of plasma transfer in the SMOLA helical open magnetic trap. The steady-state equation of matter transfer in the axially symmetric formulation contains second derivatives with respect to space. The optimal stencil for approximating the mixed derivative has been selected. For numerical implementation, the relaxation method and the more economical Seidel method were used. The dependences of the integral characteristic of the density of matter on the depth of magnetic field corrugation, the diffusion, and the plasma potential were obtained. There is a qualitative agreement between the modeled dependences and the experimental data with values of the dimensionless diffusion coefficient $D = 0.01$–0.1 and the

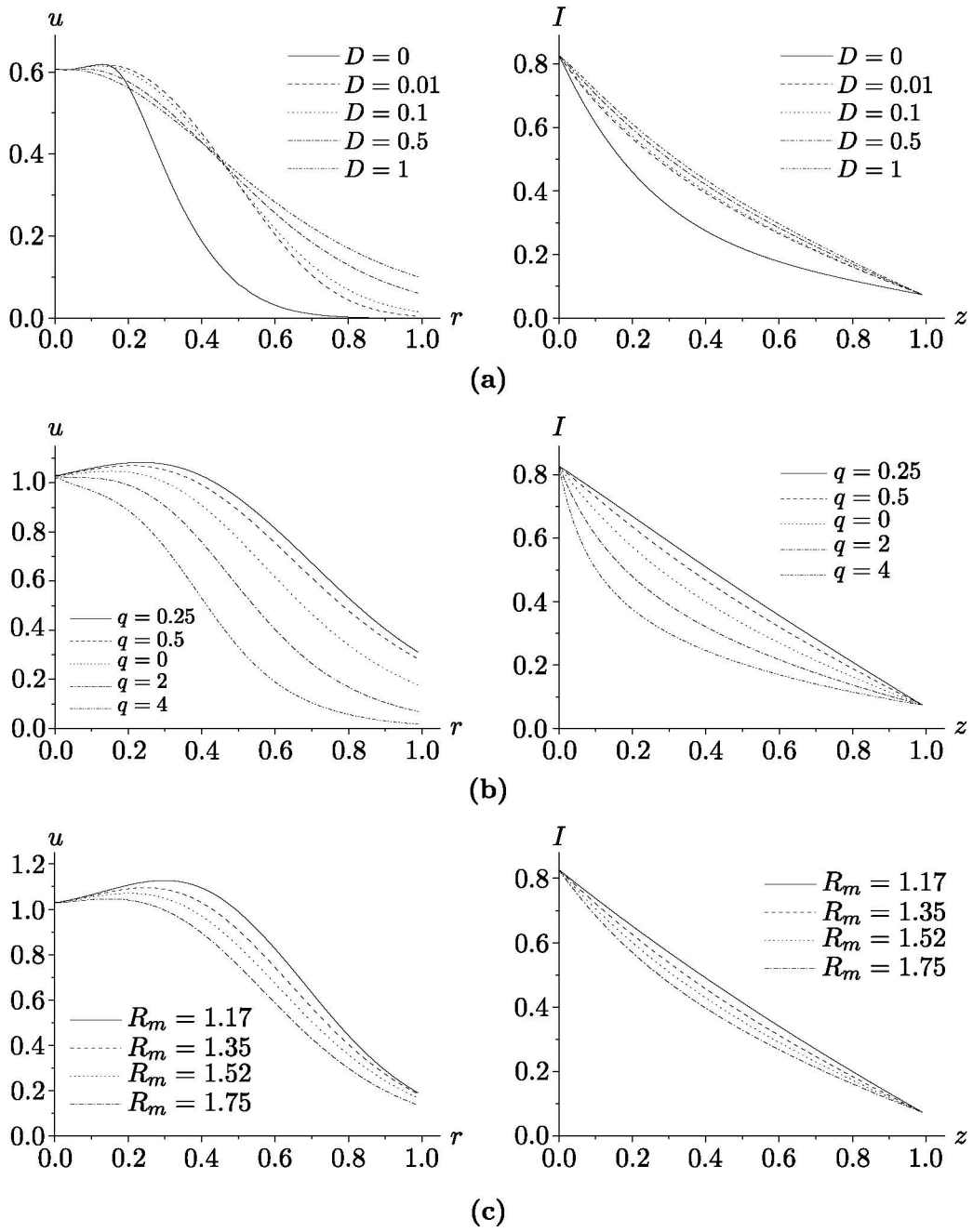

Fig. 5. Plasma concentration distribution over the cross section of the axis $z = 0.4$ (left column) and the integral of the density over the cross section (right column) for various values of the diffusion coefficient (a), the derivative of the absolute value of the electric field (b), and the corrugation depth (c).

cross-sectional average corrugation depth $R_m = 1.52$. In the calculations, the effect of pinching (reduction in the average radius) of the plasma jet is observed, which also manifests itself in the experiment. Further work will be aimed at expanding the range of parameters for which the model has sufficient predictive power.

FUNDING

The work of G.G. Lazareva and I.P. Oksogoeva was carried out with the financial support of the Ministry of Education and Science of the Russian Federation, agreement no. 075-15-2022-1115. The work of A.V. Sudnikov related to the formulation of the problem based on experimental data was

carried out with the financial support of the Russian Science Foundation, project no. 22-12-00133, https://rscf.ru/en/project/22-12-00133/.

CONFLICT OF INTEREST

The authors of this work declare that they have no conflicts of interest.

REFERENCES

1. A. A. Skovoroda, *Magnetic Traps for Plasma Confinement* (Fizmatlit, Moscow, 2019) [in Russian].
2. C. Linsmeier, B. Unterberg, J. W. Coenen, R. P. Doerner, H. Greuner, A. Kreter, and H. Maier, "Material testing facilities and programs for plasma-facing component testing," Nucl. Fusion **57** (9), 092012 (2017). https://doi.org/10.1088/1741-4326/aa4feb
3. C. B. Forest, K. Flanagan, M. Brookhart, M. Clark, C. M. Cooper, V. Dsangles, J. Egedal, D. Endrizzi, I. V. Khalzov, H. Li, M. Miesch, J. Milhone, M. Nornberg, J. Olson, E. Peterson, F. Roesler, A. Schekochihin, O. Schmitz, R. Siller, A. Spitkovsky, A. Stemo, J. Wallace, D. Weisberg, and E. Zweibel, "The Wisconsin plasma astrophysics laboratory," J. Plasma Phys. **81** (5), 345810501 (2015). https://doi.org/10.1017/S0022377815000975
4. J. D. Lawson, "Some criteria for a power producing thermonuclear reactor," Proc. Phys. Soc. **70** (1), 6–10 (1957). https://doi.org/10.1088/0370-1301/70/1/303
5. A. V. Burdakov and V. V. Postupaev, "Multiple-mirror trap: A path from Budker magnetic mirrors to linear fusion reactor," Phys.–Usp. **61** (6), 582–600 (2018). https://doi.org/10.3367/UFNe.2018.03.038342
6. P. A. Bagryansky, A. D. Beklemishev, and V. V. Postupaev, "Encouraging results and new ideas for fusion in linear traps," J. Fusion Energy **38**, 162–181 (2019). https://doi.org/10.1007/s10894-018-0174-1
7. A. D. Beklemishev, "Helicoidal system for axial plasma pumping in linear traps," Fusion Sci. Technol. **63** (1), 355–357 (2013). https://doi.org/10.13182/FST13-A16953
8. V. V. Postupaev, A. V. Sudnikov, A. D. Beklemishev, and I. A. Ivanov, "Helical mirrors for active plasma flow suppression in linear magnetic traps," Fusion Eng. Des. **106**, 29–31 (2016).
9. A. V. Sudnikov, I. A. Ivanov, A. A. Inzhevatkina, M. V. Larichkin, K. A. Lomov, V. V. Postupaev, M. S. Tolkachev, and V. O. Ustyuzhanin, "Plasma flow suppression by the linear helical mirror system," J. Plasma Phys. **88** (1), 905880102 (2022). https://doi.org/10.1017/S0022377821001276
10. A. D. Beklemishev, "Radial and axial transport in trap sections with helical corrugation," AIP Conf. Proc. **1771**, 040006 (2016). https://doi.org/10.1063/1.4964191
11. G. G. Lazareva, I. P. Oksogoeva, and A. V. Sudnikov, "Mathematical modeling of plasma transport in a helical magnetic field," Lobachevskii J. Math. **43** (10), 2685–2691 (2022). https://doi.org/10.1134/S1995080222130248
12. A. A. Samarskii and A. L. Gulin, *Numerical Methods* (Nauka, Moscow, 1989) [in Russian].
13. V. M. Volkov and E. V. Prokonina, "Difference schemes and iteration methods for multidimensional elliptic equations with mixed derivatives," Izv. NAN Belarusi. Ser. Fiz.-Mat. Nauk **54** (4), 454–459 (2018) [in Russian]. https://doi.org/10.29235/1561-2430-2018-54-4-454-459
14. A. V. Sudnikov, A. D. Beklemishev, V. V. Postupaev, A. V. Burdakov, I. A. Ivanov, N. G. Vasilyeva, K. N. Kuklin, and E. N. Sidorov, "SMOLA device for helical mirror concept exploration," Fusion Eng. Des. **122**, 86–93 (2017). https://doi.org/10.1016/j.fusengdes.2017.09.005
15. D. I. Skovorodin, I. S. Chernoshtanov, V. Kh., V. T. Astrelin, P. A. Bagryanskii, A. D. Beklemishev, A. V. Burdakov, A. I. Gorbovskii, I. A. Kotel'nikov, E. M. Magommedov, S. V. Polosatkin, V. V. Postupaev, V. V. Prikhod'ko, V. Ya. Savkin, E. I. Soldatkina, A. L. Solomakhin, A. V. Sorokin, A. V. Sudnikov, M. S. Khristo, S. V. Shiyankov, D. V. Yakovlev, and V. I. Shcherbakov, "Gas dynamic multimirror trap GDMMT," *Preprint* (Budker Inst. Nucl. Phys. Sb RAS, Novosibirsk, 2023).

16. A. A. Samarskii, V. I. Mazhukin, P. P. Matus, and G.I. Shishkin, "Monotone difference schemes for equations with mixed derivatives," Mat. Model. **13** (2), 17–26 (2001) [in Russian].

17. N. N. Yanenko, *Method of Fractional Steps for Solving Multidimensional Problems of Mathematical Physics* (Nauka, Novosibirsk, 1967) [in Russian].

18. A. A. Samarskii and E. S. Nikolaev, *Methods for Solving Grid Equations* (Nauka, Moscow, 1978) [in Russian].